Please cite the following paper at:

Sharifzadeh M, Thornhill NF, (2013). Integrated design and control using a dynamic inversely controlled process model. *Computers & Chemical Engineering*, 48, 121–134. (Link).

Integrated design and control using a dynamic inversely controlled process model

Mahdi Sharifzadeh[a,*], Nina F. Thornhill[a]

[a]Centre for Process System Engineering (CPSE), Department of Chemical Engineering, Imperial College London,

*Email: mahdi@imperial.ac.uk. Address: Department of Chemical Engineering, Imperial College London, South Kensington Campus, London SW7 2AZ.

Abstract

The profitability of chemical processes depends on their design and control. If the process design is fixed, there is little room left to improve control performance. Many commentators suggest design and control should be integrated. Nevertheless, the integrated problem is highly complex and intractable. This article proposes an optimization framework using a *dynamic inversely controlled process model*. The combinatorial complexities associated with the controllers are disentangled from the formulation, but the process and its control structure are still designed simultaneously. The new framework utilizes a multi-objective function to explore the trade-off between process and control objectives. The proposed optimization framework is demonstrated on a case study from the literature. Two parallel solving strategies are applied, and their implementations are explained. They are dynamic optimization based on i) sequential integration and ii) full discretization. The proposed integrated design and control optimization framework successfully captured the trade-off between control and process objectives.

Keywords: integrated design and control of chemical processes, stochastic mixed-integer dynamic programming, control structure selection, multi-objective optimization.

Please cite the following paper at:

Sharifzadeh M, Thornhill NF, (2013). Integrated design and control using a dynamic inversely controlled process model. *Computers & Chemical Engineering*, 48, 121–134. (Link).

1. Introduction

The current industrial practice for the design of chemical processes and their control systems is sequential in that control design is deferred until the process design is decided (Sakizlis, et al. 2010, Downs and Skogestad 2011). However, design and control share important decisions. When the process design is fixed, there is little room left for the control engineer to improve control performance. Furthermore, there are conflicts and competitions between control and process objectives, (Luyben 2004). Therefore, many commentators suggest that design and control must be integrated, (Seferlis and Georgiadis 2004).

1.1. A controller-independent framework based on perfect control

Unfortunately, addressing the integrated design and control problem using optimization poses a tough challenge for current optimization technology. Some aspects of this challenge should be attributed to controllers. Design of controllers needs decisions regarding the type of controllers (e.g. feedback, feed-forward, or model-based), pairing/partitioning of manipulated and controlled variables (i.e. the degree of centralization), and the controller parameters. In addition, including the controller model makes the mathematical model unstable and adds severe nonconvexities to the objective function and constraints, (Malcolm, et al. 2007).

Morari (1983) was among the first researchers who recognised the conceptual complexities posed by the modelling of controllers in a dynamic simulation:

"…It is generally necessary that controllers are included in the model. This often leads to arbitrary decisions about the control structure and also requires the engineer to tune these controllers interactively during the simulation, a very time consuming task. The modelled control systems are only those which are based on the experience (or ingenuity!) of the engineer doing the work. It is then impossible to distinguish if an observed poor performance is caused by some inherent plant characteristic or rather by the unfortunate choice of the control system by the engineer."

The difficulties associated with controllers have been the concerns of other researchers too. Perkins and his students (Narraway and Perkins 1993; Heath, et al. 2000; Kookos and Perkins 2004) introduced the idea of minimizing economic losses associated with back-off from active constraints. The early versions of their methodology were based on frequency domain analysis and perfect control. Later, they extended their methodology by including a generalized formulation for the controller. However, the proposed formulation was limited to linear time invariant output feedback controllers and did not include the majority of the important classes of nonlinear and model-based controllers.

Other researchers also encountered similar difficulties. For example, since static relative gain array (RGA, introduced by Bristol, 1966) does not consider transient conditions, dynamic relative gain array (DRGA) was proposed (Tung and Edgar, 1981). However, calculating the DRGA's denominator requires detailed design of controllers and *"since the DRGA is most valuable for screening alternate control system designs, the requirement of an extensive controller design tends to defeat the utility of these methods."*, (McAvoy, et al. 2003).

Furthermore, there is no general agreement between researchers on the criteria for the selection of the controller type. Some researchers (Luyben 2004; Skogestad 2009) emphasize the simplicity and robustness of the conventional multi-loop control systems and criticize the reliability and costs of modern types. On the other side of this discussion, other researchers (Stephanopoulos, and Ng 2000; Rawlings and Stewart 2008) argue the economic advantages of model-based control systems due to their systematic approach for handling constraint violations. In addition, they criticize the economic disadvantages of the constant-setpoint policy in decentralized control systems. Finally, the design of controllers at the process design stage is of limited practicality. This is because in practice, advanced controllers (e.g. MPCs) are designed using commercial packages often during process commissioning stages (Sakizlis, et al. 2010; Qin and Badgwell 2003).

To cut through these arguments, this article proposes a new optimization framework for integrated design and control, based on the notion of perfect control. The implication of perfect control assumption is that the best performance specification of a controller can be determined by the inverse solution of the process model, (Garcia and Morari1982; Morari and Zafiriou 1989). This is a well-known concept that resulted in development of a class of controllers which use the inverse of the process model as an internal element of the controller, (Skogestad and Postlethwaite 2005). Furthermore, based on this concept, a variety of controllability indices have been developed in order to quantify the causes of control imperfection, (Yuan 2011). However, no attempt has been made to incorporate the concept of perfect control into integrated design and control framework using first principle modelling and nonlinear mixed integer dynamic optimization. This paper addresses this opportunity.

1.2. Inversely controlled process models

The first step was taken in the previous publication (Sharifzadeh and Thornhill 2012), which presented a steady-state nonlinear optimization framework based on the assumption of perfect control. In that framework, a steady-state inversely controlled process model replaces the combined model of the process and its controllers. A steady-state inversely controlled process model consists of a set of nonlinear algebraic equations in which process inversion is made by fixing the controlled variables as the degrees of freedom rather than manipulated variables. The present paper develops that methodology by introducing a new modelling approach termed *dynamic inversely controlled process model*. The proposed methodology in this paper incorporates functional controllability into the optimization framework. A process is functionally controllable if for a desired vector of controlled variables, $\boldsymbol{y}(t)$, defined for $t > 0$, there exists a vector of manipulated variables, $\boldsymbol{u}(t)$, defined for $t > 0$, which generates the desired controlled variables from the initial states. In summary, while the focus of a steady-state inversely controlled process model is feasibility of initial and final states, a dynamic inversely controlled process model ensures also functional controllability, in the sense that at least one feasible control trajectory exists to take the system from the initial to the final state.

The paper is organized as follows. A novel optimization framework for integrated design and control is developed in Section 2 by modifying the conventional optimization formulation. Section 3 presents two solving strategies. They are 1) dynamic optimization based on sequential integration, and 2) dynamic optimization based on full discretization. The proposed integrated design and control framework is demonstrated on a process previously studied by Flores-Tlacuahuac and Biegler (2007). The mathematical formulation of the original case study is presented in Section 4 and is adapted to the new optimization framework in Section 5. Section 6 presents the results of the proposed optimization framework while Section 7 discusses the results. The paper ends with the conclusions in Section 8.

2. Methodology

In the subsequent sections, firstly the conventional framework for integrated design and control is presented and then modified in order to develop a new optimization framework based on perfect control.

2.1. Conventional optimization framework for integrated design and control of chemical processes

The conventional approach to integrated design and control of chemical processes can be formulated as a stochastic mixed-integer dynamic optimization (sMIDO) problem:

Please cite the following paper at:
Sharifzadeh M, Thornhill NF, (2013). Integrated design and control using a dynamic inversely controlled process model. *Computers & Chemical Engineering*, 48, 121–134. (Link).

$$min\, E\{J_s[\boldsymbol{z}(t), \boldsymbol{x}(t), \boldsymbol{u}(t), \boldsymbol{y}(t), \boldsymbol{\zeta}(t), \boldsymbol{\gamma}(t), \boldsymbol{Y_p}, \boldsymbol{Y_{cv}}, \boldsymbol{Y_{mv}}, \boldsymbol{p}, \boldsymbol{\vartheta}]\} \qquad \textbf{Problem I}$$

Subject to:

$$\boldsymbol{f}[\dot{\boldsymbol{z}}(t), \boldsymbol{z}(t), \boldsymbol{x}(t), \boldsymbol{u}(t), \boldsymbol{y}(t), \boldsymbol{Y_p}, \boldsymbol{p}, \boldsymbol{\mu_s}(t)] = 0$$

$$\boldsymbol{h}[\boldsymbol{z}(t), \boldsymbol{x}(t), \boldsymbol{u}(t), \boldsymbol{y}(t), \boldsymbol{Y_p}, \boldsymbol{p}, \boldsymbol{\mu_s}(t)] = 0$$

$$\boldsymbol{g}[\boldsymbol{z}(t), \boldsymbol{x}(t), \boldsymbol{u}(t), \boldsymbol{y}(t), \boldsymbol{Y_p}, \boldsymbol{p}, \boldsymbol{\mu_s}(t)] \leq 0$$

$$\boldsymbol{\theta}[\dot{\boldsymbol{\zeta}}(t), \boldsymbol{\zeta}(t), \boldsymbol{\gamma}(t), \boldsymbol{x}(t), \boldsymbol{z}(t), \boldsymbol{y}(t), \boldsymbol{u}(t), \boldsymbol{Y_{cv}}, \boldsymbol{Y_{mv}}, \boldsymbol{\vartheta}] = 0$$

$$\boldsymbol{\varphi}[\boldsymbol{x}(t), \boldsymbol{u}(t), \boldsymbol{y}(t), \boldsymbol{\zeta}(t), \boldsymbol{\gamma}(t), \boldsymbol{Y_{cv}}, \boldsymbol{Y_{mv}}, \boldsymbol{\vartheta}] = 0$$

$$\Omega[\boldsymbol{\mu_s}(t)] = 0$$

In the above, $\boldsymbol{z}(t)$ is the vector of process differential variables, $\boldsymbol{x}(t)$ is the vector of process algebraic variables, $\boldsymbol{u}(t)$ is the vector of candidate manipulated variables, $\boldsymbol{y}(t)$ is the vector of candidate controlled variables, $\boldsymbol{p}$ is the vector of process parameters, $\boldsymbol{\zeta}(t)$ is the vector of control differential variables, $\boldsymbol{\gamma}(t)$ is the vector of control algebraic variables, $\boldsymbol{\vartheta}$ is the vector of control parameters, $\boldsymbol{\mu_s}(t)$ is the vector of disturbance parameters. s is the index of disturbance scenario. $\boldsymbol{Y_p}$ is the vector of structural process variables. $\boldsymbol{Y_{cv}}$ and $\boldsymbol{Y_{mv}}$ are the vectors of structural variables for selection of controlled and manipulated respectively. While $\boldsymbol{Y_p}$, $\boldsymbol{Y_{cv}}$ and $\boldsymbol{Y_{cv}}$ are vectors of integer variables, the rest of the variables are continuous.

In addition, $\boldsymbol{f}[\,] = 0$ is the vector of process differential equations, $\boldsymbol{h}[\,] = 0$ is the vector of process algebraic equations, $\boldsymbol{g}[\,] \leq 0$ is the vector inequality constraints, $\boldsymbol{\theta}[\,] = 0$ is the vector of control differential equations, $\boldsymbol{\varphi}[\,] = 0$ is the vector of control algebraic equations, $\Omega[\,] = 0$ is the vector of equations for disturbances. The objective function $J_s[]$ is calculated for different disturbance scenarios s, and its expected value $E\{\}$ is minimized. The case study in Section 4 and Table 2 give physical examples of each of these categories of variables and equations.

The above mathematical formulation applies a combined modelling approach in which the models of the process and its controllers are included and linked together. The concept is shown in Fig. 1 that shows candidate optimization variables being exported by the optimization algorithm to the combined model which is shown by the dotted envelope. Then, the combined model is fixed and its performance is tested under different disturbances and reported to the optimization algorithm. The optimization algorithm evaluates the termination criteria and decides on improvement of the optimization variables.

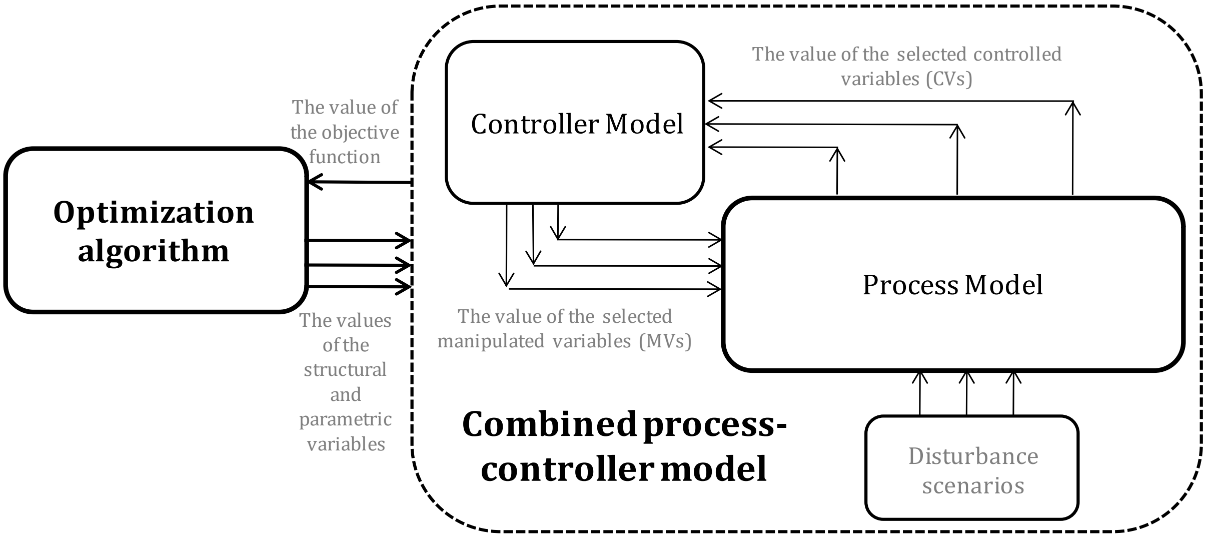

Fig. 1. The conventional optimization framework for integrated design and control of chemical processes.

Please cite the following paper at:

Sharifzadeh M, Thornhill NF, (2013). Integrated design and control using a dynamic inversely controlled process model. *Computers & Chemical Engineering*, 48, 121–134. (Link).

2.2. A novel optimization framework using inversely controlled process model

The aim of the analysis in this section is to disentangle the complexities associated with controllers from the conventional optimization framework.

2.2.1. Perfect control and the inversely controlled process model

One way of incorporating perfect control into the integrated design and control framework is to embed an inverse-based controller. For example, the methods of nonlinear feedback linearizing controller enable analytical synthesis of the controller by identifying an invertible mapping which transforms the nonlinear formulation into a linear and controllable formulation, (Daoutidis and Kravaris 1991, 1992a, 1994; Hangos, et al., 2004). Such a transformation may guarantee some desirable properties (e.g. minimum-phase behaviour) of the system.

However, these methods might not be appropriate for integrated design and control because they are based on the assumption that manipulated variables (MVs) and controlled variables (CVs) are known in advance. As a result, for each combination of MVs, and CVs, a set of nonlinear feedback linearizing controllers needs to be synthesized analytically, which if not infeasible, would be a very tedious task. Furthermore, including these controllers in the mathematical superstructure would increase the size of the optimization problem to be even larger than the conventional framework including decentralized controllers.

Therefore, in this research instead of using any inverse-based controller (e.g., IMCs, nonlinear feedback linearizing controllers), the model of controllers is replaced by perfect control equations which invert the process model, and then the resulted inversely controlled process model (including structural variables for selecting MVs and CVs) is optimized using mixed integer dynamic programming.

In order to disentangle the design of controllers, their algebraic and differential equations ($\boldsymbol{\theta}[] = 0$ and $\boldsymbol{\varphi}[] = 0$) must be replaced by perfect control equations which ensure that the selected controlled variables are constant at their desired values:

$$y_i(t) = y_{i,setpoint} \qquad (1)$$

where $y_i(t)$ is the selected controlled variable and $y_{i,setpoint}$ is the corresponding desired setpoint. In principle, $y_{i,setpoint}$ can be time-dependent. However, in optimization of a continuous process it would normally be constant, equivalent to disturbance rejection, which is the focus of this research. These considerations can be formulated using mixed-integer programming:

$$min \sum_{s=1}^{n_s} L_s \times J_s(\boldsymbol{z}(t), \boldsymbol{x}(t), \boldsymbol{u}(t), \boldsymbol{y}(t), \mu_s(t), \boldsymbol{Y_p}, \boldsymbol{Y_{cv}}, \boldsymbol{Y_{mv}}, \boldsymbol{p}, \boldsymbol{y_{i,setpoint}}) \qquad \textbf{Problem II}$$

subject to:

$$\boldsymbol{f}[\dot{\boldsymbol{z}}(t), \boldsymbol{z}(t), \boldsymbol{x}(t), \boldsymbol{u}(t), \boldsymbol{y}(t), \boldsymbol{Y_p}, \boldsymbol{p}, \boldsymbol{\mu_s}(t)] = 0$$

$$\boldsymbol{h}[\boldsymbol{z}(t), \boldsymbol{x}(t) , \boldsymbol{u}(t), \boldsymbol{y}(t), \boldsymbol{Y_p}, \boldsymbol{p}, \boldsymbol{\mu_s}(t)] = 0$$

$$\boldsymbol{g}[\boldsymbol{z}(t), \boldsymbol{x}(t), \boldsymbol{u}(t), \boldsymbol{y}(t), \boldsymbol{Y_p}, \boldsymbol{p}, \boldsymbol{\mu_s}(t)] \le 0$$

$$\Omega[\boldsymbol{\mu_s}(t)] = 0$$

$$\boldsymbol{Y_{cv,i}} \times \left(\boldsymbol{y_i}(t) - \boldsymbol{y_{i,setpoint}}\right) = 0$$

$$(\boldsymbol{1} - \boldsymbol{Y_{mv,j}}) \times \left(\boldsymbol{u_j}(t) - \boldsymbol{u_{j,nominal}}\right) = 0$$

$$\sum_{i=0}^{I_{kcv}} \boldsymbol{Y_{cv,i}} = dof, \qquad \boldsymbol{Y_{cv,i}} \in \{0, 1\}$$

$$\sum_{j=0}^{I_{kmv}} \boldsymbol{Y}_{\boldsymbol{mv},\boldsymbol{j}} = dof\,, \qquad \boldsymbol{Y}_{\boldsymbol{mv},\boldsymbol{j}} \in \{0,1\}$$

In Problem II, the expected value of the objective function is represented using the likelihood L_s of the individual objective values, J_s, calculated for each disturbance scenario, s. n_s is the total number of disturbance scenarios. $\boldsymbol{Y}_{\boldsymbol{cv},\boldsymbol{i}}$ and $\boldsymbol{Y}_{\boldsymbol{mv},\boldsymbol{j}}$ are binary variables, which denote whether a controlled variable or a manipulated variable is selected, respectively. Notice that for the manipulated variable, the multiplier encloses the complement of the corresponding binary variable, i.e. $(\boldsymbol{1}-\boldsymbol{Y}_{\boldsymbol{mv},\boldsymbol{j}})$. The implication is that if a manipulated variable is not selected, it remains at its nominal value, while the required value of the selected manipulated variable is calculated using the inversely controlled process model. The last two constraints ensure that the selected control structure is consistent according to the available degrees of freedom, dof. For each available degree of freedom, the optimizer may choose from a set of candidate controlled and manipulated variables. The numbers of options for a controlled variable or a manipulated variable are represented by I_{kcv} and I_{kmv}, respectively.

The value of the objective function depends on the disturbances (Halvorsen, et al. 2003). In this research, the stochastic optimization Problem I is addressed using a multi-period optimization. The value of the objective function is constructed by adding individual objective functions for different disturbance scenarios weighted by the likelihood of each disturbance scenario.

Fig. 2 shows the concept. The models of the controllers have been replaced with equations representing perfect control, which enable the directions of the information flows to be reversed from the controlled variables to the manipulated variables. The values of the controlled variables are maintained constant by perfect control equations while the time trajectories of the manipulated variables are adjusted in order to reject the disturbances. Then, the values of the objective function and constraints can be evaluated and reported to the optimization algorithm. The optimization algorithm evaluates the termination criteria and decides on improvement of the optimization variables.

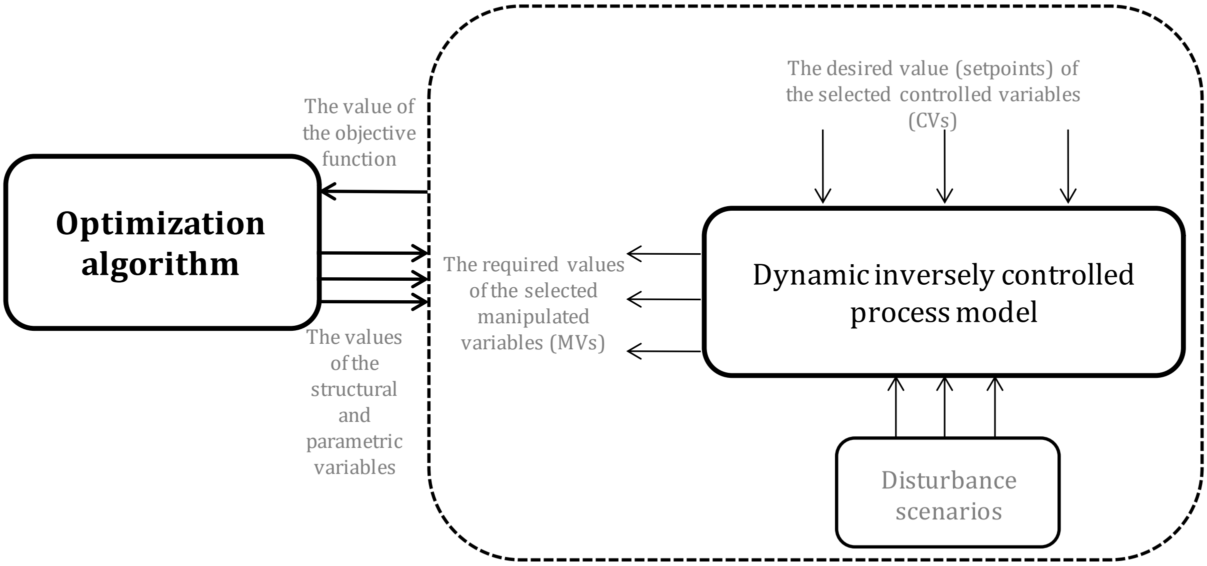

Fig. 2. The proposed integrated design and control framework using the inversely controlled process model.

Please cite the following paper at:
Sharifzadeh M, Thornhill NF, (2013). Integrated design and control using a dynamic inversely controlled process model. *Computers & Chemical Engineering*, 48, 121–134. (Link).

3. Solving strategies and implementation techniques

This section presents two solving strategies for Problem II. The first solving strategy is the classical dynamic optimization method based on sequential integration over time. The second solving strategy is based on full discretization of time-dependent variables. Both solving strategies are applied to the case study of Section 4. More detail about these solving strategies can be found in literature, (Biegler 2010; Avraam, et al. 1998, 1999; Sharif, et al. 1998 ; Mohideen, et al. 1997, Schweiger and Floudas, 1997; Bansal, et al. 2000, 2003).

3.1. Dynamic optimization based on sequential integration strategy

In the sequential strategy of a conventional integrated design and control framework (Problem I), input variables, $\boldsymbol{u}(t)$, are parameterized in order to determine the optimal trajectory. However, in the inversely controlled process model (Fig. 2), the controlled variables $\boldsymbol{y}(t)$ (outputs of the conventional problem) represent the input variables of the dynamic optimization problem and are parameterized by the desired setpoints, i.e., $\boldsymbol{y_{i,setpoint}}$ using perfect equation (1). By the parameterization of the controlled variables, Problem II can be summarized as the following nonlinear program:

$$min \sum_{s=1}^{n_s} L_s \times J_s\left(\boldsymbol{\mu_s}(t), \boldsymbol{Y_p}, \boldsymbol{Y_{cv,}}, \boldsymbol{Y_{mv,}}, \boldsymbol{p}, \boldsymbol{y_{i,setpoint}}\right) \qquad \textbf{Problem III} - \textbf{A}$$

subject to:

$$\boldsymbol{f}[\dot{\boldsymbol{z}}(t), \boldsymbol{z}(t), \boldsymbol{x}(t), \boldsymbol{u}(t), \boldsymbol{y}(t), \boldsymbol{Y_p}, \boldsymbol{p}, \boldsymbol{\mu_s}(t)] = 0$$

$$\boldsymbol{h}[\boldsymbol{z}(t), \boldsymbol{x}(t) , \boldsymbol{u}(t), \boldsymbol{y}(t), \boldsymbol{Y_p}, \boldsymbol{p}, \boldsymbol{\mu_s}(t)] = 0$$

$$\boldsymbol{g}[\boldsymbol{z}(t), \boldsymbol{x}(t), \boldsymbol{u}(t), \boldsymbol{y}(t), \boldsymbol{Y_p}, \boldsymbol{p}, \boldsymbol{\mu_s}(t)] \le 0$$

$$\Omega[\boldsymbol{\mu_s}(t)] = 0$$

$$\boldsymbol{Y_{cv,i}} \times \left(\boldsymbol{y_i}(t) - \boldsymbol{y_{i,setpoint}}\right) = 0$$

$$(\boldsymbol{1} - \boldsymbol{Y_{mv,j}}) \times \left(\boldsymbol{u_j}(t) - \boldsymbol{u_{j,nominal}}\right) = 0$$

$$\sum_{i=0}^{I_{kcv}} \boldsymbol{Y_{cv,i}} = dof, \qquad \boldsymbol{Y_{cv,i}} \in \{0, 1\}$$

$$\sum_{j=0}^{I_{kmv}} \boldsymbol{Y_{mv,j}} = dof\ , \qquad \boldsymbol{Y_{mv,j}} \in \{0, 1\}$$

The information flow in the sequential solving strategy is presented in Fig. 3 and explained as follows. In a sequential dynamic optimization strategy, an embedded DAE solver provides objective function information to a nonlinear optimization solver.

At a given iteration of the optimization cycle,

Step 1. The nonlinear optimization algorithm specifies the values of the optimization variables.

Step 2. The steady-state inversely controlled process model (the lower left-hand block in Fig. 3) evaluates the feasibility of steady-state process inversion for the disturbance scenarios. This is because the integration of DAE system must be initialized from a feasible steady-state condition.

Step 3. In the case that feasible steady states cannot be found, the algebraic equation (AE) solver reports a failure to the nonlinear optimization algorithm to change the values of optimization variables, either by reducing the step size of the nonlinear optimizer or by adding an incremental random number to the current solution. Return to Step 1.

Step 4. For the fixed values of these variables, the Problems III-A is an initial value problem and the DAE system can be solved by numerical integration. The controlled variables are parameterized by equation (1) and the sequential integration gives the time trajectory for the manipulated variables and the remaining state variables.

Step 5. Based on the values of the objective function and the constraints, the optimization algorithm makes decisions regarding the termination of the optimization cycle or improving the values of the optimization variables by returning to Step 1.

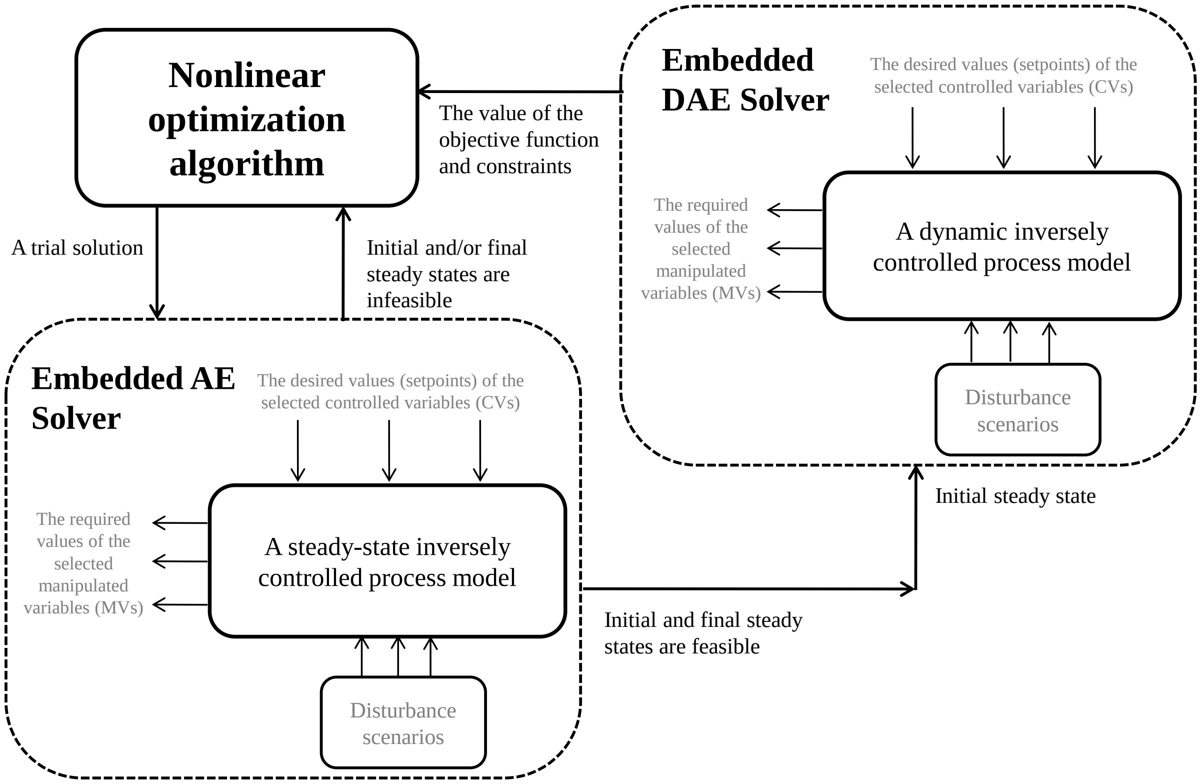

Fig. 3. The sequential solving strategy for the proposed integrated design and control framework.

3.2. Dynamic optimization based on full discretization strategy

The second solving strategy was based on full discretization of differential and algebraic variables using the Radau collocation method. The use of Radau polynomials ensures that the collocation variables have the same bounds as the corresponding differential and algebraic variables, (Biegler 2010). After full discretization, the mixed-integer nonlinear dynamic optimization problem is translated into a large mixed-integer nonlinear optimization problem, which can be solved using conventional MINLP methods. The equivalent discretized version of Problem III-A is as follows:

$$min \sum_{s=1}^{n_s} L_s \times J_s(\boldsymbol{z_{ij}}, \boldsymbol{x_{ij}}, \boldsymbol{u_{ij}}, \boldsymbol{y_{ij}}, \boldsymbol{\mu_{ij,s}}, \boldsymbol{Y_p}, \boldsymbol{Y_{cv}}, \boldsymbol{Y_{mv}}, \boldsymbol{p}, \boldsymbol{y_{i,setpoint}}) \qquad \textbf{Problem III} - \textbf{B}$$

Subject to:

$$\boldsymbol{f}[\boldsymbol{z_{ij}}, \boldsymbol{x_{ij}}, \boldsymbol{u_{ij}}, \boldsymbol{y_{ij}}, \boldsymbol{Y_p}, \boldsymbol{p}, \boldsymbol{\mu_{ij,s}}] = 0$$

$$\boldsymbol{h}[\boldsymbol{z_{ij}}, \boldsymbol{x_{ij}}, \boldsymbol{u_{ij}}, \boldsymbol{y_{ij}}, \boldsymbol{Y_p}, \boldsymbol{p}, \boldsymbol{\mu_{ij,s}}] = 0$$

$$\boldsymbol{g}[\boldsymbol{z_{ij}}, \boldsymbol{x_{ij}}, \boldsymbol{u_{ij}}, \boldsymbol{y_{ij}}, \boldsymbol{Y_p}, \boldsymbol{p}, \boldsymbol{\mu_{ij,s}}] \leq 0$$

$$\Omega[\boldsymbol{\mu_{ij,s}}] = 0$$

$$\boldsymbol{Y_{cv,i}} \times (\boldsymbol{y_{ij}} - \boldsymbol{y_{setpoint}}) = 0$$

$$(\mathbf{1} - \boldsymbol{Y_{mv,j}}) \times (\boldsymbol{u_{ij}} - \boldsymbol{u_{nominal}}) = 0$$

$$\sum_{i=0}^{I_{kcv}} \boldsymbol{Y_{cv,i}} = dof, \qquad \boldsymbol{Y_{cv,i}} \in \{0,1\}$$

$$\sum_{j=0}^{I_{kmv}} \boldsymbol{Y_{mv,j}} = dof\,, \qquad \boldsymbol{Y_{mv,j}} \in \{0,1\}$$

where $\boldsymbol{z_{ij}}, \boldsymbol{x_{ij}}, \boldsymbol{u_{ij}}$, and $\boldsymbol{y_{ij}}$ are collocation optimization variables. In this solving strategy, the continuity equations in addition to the differential and algebraic equations at the initial point ensure consistent initialization of the integrated design and control framework. The model inversion is performed by including perfect control equations in the optimization constraints.

4. Case study for the conventional integrated design and control optimization framework

Flores-Tlacuahuac and Biegler (2007) studied a process comprising two series heat-integrated reactors in order to benchmark the performance of different solving strategies for mixed-integer dynamic optimization. The cooling system of the process may have either co-current or counter-current heat exchangers which are shown in Figs. 4a and b, respectively. The mathematical formulation of their study is presented in this section and matches the optimization framework of Fig. 1. In Section 5, this mathematical formulation will be modified and adapted to the new optimization framework using an inversely controlled process model.

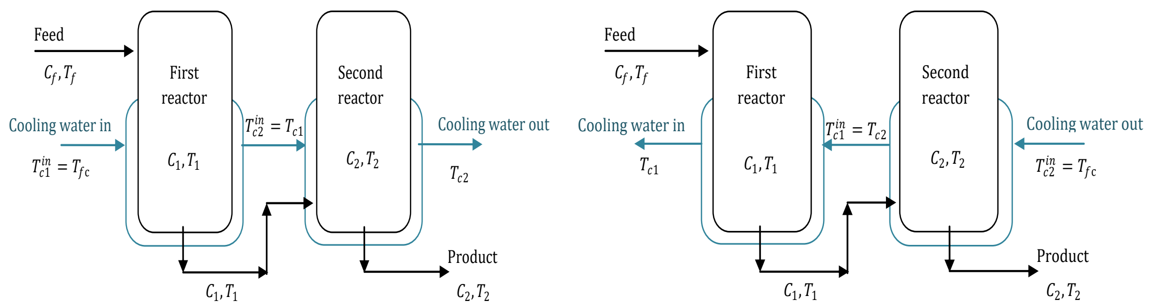

Figs. 4. Different process structures: a) the co-current structure b) the counter-current structure.

The justification for the choice of the case study in the present research was to be illustrative and reproducible. For this reason, comprehensive details of the case study and implementation techniques are presented. The case of two heat-integrated series reactors however, is a highly nonlinear process as discussed by Flores-Tlacuahuac and Biegler (2007).

It is notable that as discussed by other researchers, *"Simultaneous optimization of design and control structure along with control tuning in an infinite uncertain space poses a tough challenge for current optimization technology"*, (Malcolm, et al. 2007). Therefore, the effectiveness of the proposed optimization framework should be measured and compared to the conventional optimization framework. As will be seen, the advantages of the proposed optimization framework include reducing the size of the optimization problem and ensuring the independency of the results from a specific controller type, which suggest a lower level of numerical and conceptual complexities compared to the conventional optimization framework for integrated design and control.

The mass and energy balances of the first and the second reactors are presented by equations (2) to (9). The definitions of the variables and the value of the design parameters are reported in Table 1.

The mass and energy balances for the first reactor are:

$$\frac{dC_1}{dt} = \frac{C_f - C_1}{\theta_1} + r_{A1} \qquad (2)$$

$$\frac{dT_1}{dt} = \frac{T_f - T_1}{\theta_1} + \beta \times r_{A1} - \alpha_1 \times (T_1 - T_{c1}) \qquad (3)$$

The energy balance for the cooling jacket of the first reactor is:

$$\frac{dT_{c1}}{dt} = \frac{T_{C1}^{in} - T_{C1}}{\theta_{c1}} + \alpha_{c1} \times (T_1 - T_{c1}) \qquad (4)$$

The mass and energy balances for the second reactor are:

$$\frac{dC_2}{dt} = \frac{C_1 - C_2}{\theta_2} + r_{A2} \qquad (5)$$

$$\frac{dT_2}{dt} = \frac{T_1 - T_2}{\theta_2} + \beta \times r_{A2} - \alpha_2 \times (T_2 - T_{c2}) \qquad (6)$$

The energy balance for the cooling jacket of the second reactor is:

$$\frac{dT_{c2}}{dt} = \frac{T_{c2}^{in} - T_{c2}}{\theta_{c2}} + \alpha_{c2} \times (T_2 - T_{c2}) \qquad (7)$$

The parameters in equations (13)-(18) are:

$$\theta_1 = \frac{V_1}{Q}, \quad \theta_2 = \frac{V_2}{Q}, \quad \alpha_1 = \frac{U \times A_1}{\rho \times V_1 \times C_p}, \quad \alpha_2 = \frac{U \times A_2}{\rho \times V_2 \times C_p}$$

$$\theta_{c1} = \frac{V_{c1}}{Q_c}, \quad \theta_{c2} = \frac{V_{c2}}{Q_c}, \alpha_{c1} = \frac{U \times A_1}{\rho_c \times V_{c1} \times C_{pc}}, \alpha_{c2} = \frac{U \times A_2}{\rho_c \times V_{c2} \times C_{pc}}, \beta = \frac{\Delta Hr}{\rho \times C_p}$$

The following kinetic relations represent the reaction rates:

$$r_{A1} = -K_0 \times e^{-E/R \times T_1} \times C_1 \qquad (8)$$

$$r_{A2} = -K_0 \times e^{-E/R \times T_2} \times C_2 \qquad (9)$$

The decisions regarding the process structure is represented by the binary variable Y_p in the equations (10) and (11):

$$T_{c1}^{in} = Y_p \times T_{fc} + (1 - Y_p) \times T_{c2} \qquad (10)$$

$$T_{c2}^{in} = Y_p \times T_{c1} + (1 - Y_p) \times T_{fc} \qquad (11)$$

$$\begin{cases} Y_p = 1 & \text{co} - \text{current configuration} \\ Y_p = 0 & \text{countercurrent configuration} \end{cases}$$

The equations for the controller model are:

$$T_f = T_{f,nominial} + (1 - Y_{mv}) \times (K_P \times P(t) + K_i \times I(t)) \qquad (12)$$

$$Q_c = Q_{c,nominial} - Y_{mv} \times (K_P \times P(t) + K_i \times I(t)) \qquad (13)$$

$$P(t) = Y_{cv} \times (T_{1,setpoint} - T_1) + (1 - Y_{cv}) \times (T_{2,setpoint} - T_2) \qquad (14)$$

$$\frac{dI(t)}{dt} = P(t), \qquad I(0) = 0 \qquad (15)$$

$$\begin{cases} Y_{mv} = 1 & Q_c \text{ is selected as the mnaipulated variable} \\ Y_{mv} = 0 & T_f \text{ is selected as the mnaipulated variable} \end{cases}$$

$$\begin{cases} Y_{cv} = 1 & T_1 \text{ is selected as the mnaipulated variable} \\ Y_{cv} = 0 & T_2 \text{ is selected as the mnaipulated variable} \end{cases}$$

In the original case study presented by Flores-Tlacuahuac and Biegler (2007), the following objective function was introduced:

$$min \frac{1}{t_{final}} \int_{0}^{tfinal} \left(T_{i,setpiont} - T_i\right)^2 dt \qquad i \in \{1,2\} \qquad (16)$$

Table 1
The parameters and the values of the variables at the base case scenario

Parameter	Description	Value*	Unit *	Value	SI Unit
Q	Volumetric feed flow rate	2.5	$L.s^{-1}$	2.5×10^{-3}	$m^3.s^{-1}$
T_f	Feed stream temperature	29	^oC	302	K
C_f	Feed Stream concentration	0.6	$mol.L^{-1}$	0.6	$kmol.m^{-3}$
V_1	Volume of the first reactor	900	L	0.9	m^3
V_2	Volume of the second reactor	900	L	0.9	m^3
Q_c	Cooling water flow rate	2	$L.s^{-1}$	2×10^{-3}	$m^3.s^{-1}$
T_{fc}	Cooling water feed stream temperature	25	^oC	298	K
V_{c1}	Volume of the cooling jacket of the first reactor	100	L	0.1	m^3
V_{c2}	Volume of the cooling jacket of the second reactor	100	L	0.1	m^3
E	Activation energy	10.1	$kcal.mol^{-1}$	4.2×10^7	$J.kmol^{-1}$
K_0	Pre-exponential factor	2000	s^{-1}	2000	s^{-1}
R	Ideal gas constant	0.00198	$kcal.mol^{-1}.K^{-1}$	8.32×10^3	$J.kmol^{-1}.K^{-1}$
ρ	Products density	850	$g.L^{-1}$	850	$kg.m^{-3}$
C_p	Product heat capacity	0.000135	$kcal.g^{-1}.C^{-1}$	564.84	$J.kg^{-1}.C^{-1}$
ΔH_r	Heat of reaction	−35	$kcal.mol^{-1}$	-1.46×10^8	$J.kmol^{-1}$
ρ_c	Cooling water density	1000	$g.L^{-1}$	1000	$kg.m^{-3}$
C_{pc}	Cooling water heat capacity	0.001	$kcal.g^{-1}.C^{-1}$	4.2×10^3	$J.kg^{-1}.K^{-1}$
A	Heat transfer area	900	cm^2	0.09	m^2
U	Heat transfer coefficient	0.00004	$kcal.s^{-1}.cm^{-2}.C^{-1}$	1.7×10^3	$J.s^{-1}.m^{-2}.K^{-1}$

* Values by Flores-Tlacuahuac and Biegler (2007).

5. Application of integrated design and control framework using a dynamic inversely controlled process model

This section gives some necessary extensions to the case study and develops the dynamic inversely controlled process model for this process. Other topics include explaining controllability constraints, a method for comparison of a combined process-controller model with the inversely controlled process model, a discussion about the objective function of the integrated design and control framework and explanation of the implementation techniques.

5.1. Amendments to the original case study

Flores-Tlacuahuac and Biegler (2007) considered a fixed value for the heat transfer area A_i , $i = 1{,}2$ of each cooling jacket. However, it is usual to scale the heat transfer area of a cooling jacket with reactor volume by:

$$A_i = coef \times (V_i)^{2/3} \tag{17}$$

Therefore, equation (17) is added to the original case study and its coefficient is calculated from the base-case design shown in Table 1, resulting in $coef = 9.655$ cm^2.L$^{(-2/3)}$. The base case design requires a heat transfer area that is much smaller than the surface area of the reactor. Such a configuration would have to be realized in practice by a jacket that makes only partial contact with the reactor walls.

Flores-Tlacuahuac and Biegler (2007) suggested 50% and 200% as the lower and upper bounds for the optimization values. The upper and lower bounds for the optimization variables used instead in this research are 50% and 300%. The reason is that for some specific structures the heat transfer is thermodynamically limited by the maximum allowable temperature of the cooling water exiting the process, which is 80^{o}C.

Flores-Tlacuahuac and Biegler (2007) assumed that the two reactors and their cooling jackets are identical. This restrictive assumption is relaxed in the present research in order to provide extra degrees of freedom for the integrated design and control optimization.

Flores-Tlacuahuac and Biegler (2007) assumed the disturbance to be the feed composition. They evaluated several disturbances in the range $C_f = 0.55$ kmol.m^{-3} to $C_f = 0.65$ kmol.m^{-3} with different time constants. In this research a step disturbance from $C_f = 0.55$ kmol.m^{-3} to $C_f = 0.65$ kmol.m^{-3} is considered a likely operational condition. This disturbance covers all the operational regions explored by the disturbances in the original case study (Flores-Tlacuahuac and Biegler 2007). However, due to nonlinearity of the process the direction of the disturbance may be important. Therefore, this paper also considers another disturbance with the same magnitude but the reverse direction from $C_f = 0.65$ kmol.m^{-3} to $C_f = 0.55$ kmol.m^{-3}. It is assumed that these disturbances have the same likelihood.

5.2. Inversely controlled process model for the case of two series reactors

This section discusses replacement of the controller model with the perfect control equations and inverting the process model. The structural control decision regarding the selection of controlled variables is represented by the binary variable Y_{cv} as follows:

$$Y_{cv} \times T_1 = Y_{cv} \times T_{1,setpoint} \tag{18a}$$

$$(1 - Y_{cv}) \times T_2 = (1 - Y_{cv}) \times T_{2,setpoint} \tag{18b}$$

$$\begin{cases} Y_{cv} = 1 & T_1 \text{ is selected as controlled variable} \\ Y_{cv} = 0 & T_2 \text{ is selected as controlled variable} \end{cases}$$

The perfect control equations (18) represent a high index formulation, which after index reduction are:

$$Y_{cv} \times \frac{\partial T_1}{\partial t} = 0 \tag{19a}$$

$$(1 - Y_{cv}) \times \frac{\partial T_2}{\partial t} = 0 \tag{19b}$$

$$\begin{cases} T_1(t_{initial}) = T_{1,setpoint} \\ T_2(t_{initial}) = T_{2,setpoint} \end{cases}$$

$$\begin{cases} Y_{cv} = 1 & T_1 \text{ is selected as controlled variable} \\ Y_{cv} = 0 & T_2 \text{ is selected as controlled variable} \end{cases}$$

Please cite the following paper at:
Sharifzadeh M, Thornhill NF, (2013). Integrated design and control using a dynamic inversely controlled process model. *Computers & Chemical Engineering*, 48, 121–134. (Link).

More discussion on index reduction is presented in Section 7.2.1.The structural control decision regarding the selection of manipulated variables is represented by binary variable Y_{mv} as follows:

$$Y_{mv} \times T_f = Y_{mv} \times T_{f,nominial} \tag{20a}$$

$$(1 - Y_{mv}) \times Q_c = (1 - Y_{mv}) \times Q_{c,nominial} \tag{20b}$$

$$\begin{cases} Y_{mv} = 1 & Q_c \text{ is selected as manipulated variable} \\ Y_{mv} = 0 & T_f \text{ is selected as manipulated variable} \end{cases}$$

These equations ensure that the manipulated variable which is not selected will be maintained constant at its nominal value, but the selected manipulated variable is free and available to the optimizer.

In conclusion, the mathematical formulation used for integrated design and control of the case study consists of equations (2-11, 19, 20). Table 2 matches the case study formulation with the problem formulations III-A & B. The other terms of equations (2-11, 19, 20) not shown in this table are variables which are combination of other variables.

Table 2.
The correspondence of the two solving strategies with the case study formulation.

Solving strategy	Sequential integration	Full discretization
Enumeration variables	Y_p, Y_{cv}, Y_{mv}	none
Time-independent optimization variables	$V_1, V_2, V_{c1}, V_{c2}, T_{i,setpoint}$	$Y_p, Y_{cv}, Y_{mv}, V_1, V_2, V_{c1}, V_{c2}, T_{i,setpoint}$
Time-dependent optimization variables	DAE solver variables: C_1, C_2, C_f $T_1, T_2, T_f,$ $T_{c1}, T_{c2}, T_{c1}^{in}, T_{c2}^{in},$ r_{A1}, r_{A2}, Q_c	Discretization variables: 1) differential collocation variables: $C_{1,ij}, C_{2,ij}, T_{1,ij}, T_{2,ij}, T_{c1,ij}, T_{c2,ij},$ 2) algebraic collocation variables: $C_{f,ij}, T_{f,ij}, T_{c1,ij}, T_{c2,ij}, T_{c1,ij}^{in}, T_{c2,ij}^{in},$ $r_{A1,ij}, r_{A2,ij}, Q_{c,ij}$
Differential constraints: $\boldsymbol{f}[]$	Equations (2-7)	Equations (2-7)
Algebraic constraints: $\boldsymbol{h}[]$	Equations (8-11, 19, 20)	Equations (8-11, 19, 20)

Note: The multi-objective function of the case study in the new framework is explained in Section 5.3.

5.3. Multi-objective function

In the original case study by Flores-Tlacuahuac and Biegler (2007), the objective function was equation (16). This objective function is not appropriate for the new integrated design and control framework for two reasons. Firstly, it does not include any term for process objectives (e.g., required capital investment). Therefore, this objective function contradicts with the aim of integrated design and control framework to establish a trade-off between control and process objectives. Secondly, minimizing the controller error (i.e., difference in the actual and desired values of controlled variables) is not the concern of perfect control because due to satisfaction of equation (1), the integral of the square of controller error (ISE) is already equal to zero:

$$ISE_i = \int (\boldsymbol{T_i} - \boldsymbol{T_{i,setpoint}})^2 dt = 0 \tag{21}$$

However, in the case study, the temperature is being controlled to inferentially control the composition of the second reactor. The difference between the actual and desired compositions of the second reactor gives a rigorous measure of the success of inferential control. This measure was included in the new multi-objective function for the integrated design and control framework, and is discussed in the following along with other competing objectives.

Luyben (2004) recognized conflicts and competitions between process and control objectives. He gave a list of examples where improving a process objective degrades a competing control objective. In this research, the following multi-objective function is considered in order to capture the trade-off between control and process objectives:

$$min \sum_{s=1,2} L_s \times J_s[\,] \tag{22}$$

$$J_s[\,] = w'_1 \times ControlObjectives + w'_2 \times ProcessObjectives$$

$$ControlObjectives = w_1 \times obj_1 + w_2 \times obj_2$$

$$ProcessObjectives = 1 \times obj_3 + 1.5 \times obj_4$$

$$obj_1 = \int_{t0}^{tfinal} \left|C_2 - C_{2,desired}\right| dt, \qquad [obj_1] = \mathrm{kmol.m^{-3}.s}$$

$$obj_2 = \int_{t0}^{tfinal} \left(\frac{|MV - MV_{nominal}|}{MV_{nominal}}\right) dt, \qquad [obj_2] = \mathrm{s}$$

$$obj_3 = \sum_{i=1}^{2} V_i, \qquad [obj_3] = \mathrm{m^3}$$

$$obj_4 = \sum_{i=1}^{2} V_{c,i}, \qquad [obj_4] = \mathrm{m^3}$$

The terms of the multi-objective function (22) represent two different categories of objectives for integrated design and control; the first category concerns control objectives and the second category concerns process objectives. In the first category, there are two control objectives. The first one, obj_1, measures the success of the control structure in controlling the concentration of the second reactor inferentially by controlling the temperature of either the first or the second reactors. In the original case study (Flores-Tlacuahuac and Biegler 2007), the aim of integrated design and control was to maximize the conversion. Therefore, $C_{2,desired}$ is set equal to zero in this research to minimize the loss of the reactant. The weighting factor of the first objective, w_1, can be interpreted as the costs of the lost reactant over the simulation time. The second objective,obj_2, measures the costs of the control action. This variable is scaled by its nominal value because different manipulated variables may have different dimensions. The physical implication of this objective is that when disturbances are imposed, maintaining the controlled variable at its setpoint should requires minimum changes in the manipulated variable (Qin and Badgwell 2003; McAvoy 1999). Excessive changes in the manipulated variables are undesirable as they may invoke interactions with other control loops. In addition, aggressive application of the control action lead to earlier equipment failure, and would increase maintenance costs. The weighting factor of the second objective, w_2, can be interpreted as the costs of changing the manipulated variable over the simulation time. The third and the fourth objective functions obj_3 and obj_4 are objectives for process design, and represent the required investment capital for purchasing the reactors and their cooling jackets. Their weighting factors have the dimension of cost per unit of volume.

In the absence of any data for the case study, in order to explore the trade-off between the process objectives and the control objectives some simplifying assumptions are made and the weighting factor w_i are fixed and then the trade-off between the control objectives and the process objectives are explored by changing the ratio of w'_1 and w'_2.

In this research, $w_1 = 1$ and $w_2 = 0.01$ give an estimate of the relative importance of first and second control objectives. In the process objective, it is assumed that the cooling jackets are 50% more expensive than the reactors, because they are more prone to thermal shocks, and have higher manufacturing costs due to their shape, size and hydraulic considerations. In order

Please cite the following paper at:
Sharifzadeh M, Thornhill NF, (2013). Integrated design and control using a dynamic inversely controlled process model. *Computers & Chemical Engineering*, 48, 121–134. (Link).

to explore the trade-off between the control objectives and the process objectives the ratio between their weighting factors, w'_1 and w'_2 , needs to be changed. In this research, the optimization is performed for a variety of weighting factors $w'_1 \in \{1\}$, and $w'_1 \in \{10^{-6}, 10^{-3}, 3 \times 10^{-3}, 5 \times 10^{-3}, 10^{-2}\}$. These values correspond to a domain where the control objectives and the process objectives compete with each other.

In this research, the value of $t_{final} = 1000$ s is considered, which was large enough that most of intermediate solutions reached their final steady states. The choice of the number of time-intervals determines the precision of the simulation and was specified using pre-optimization analysis. For sequential solving strategy, the integration step size was 10s and for the full discretization strategy, the length of the finite elements was 25s. It is assumed that the disturbances have equal likelihood ($L_1 = L_2 = 0.5$). Both solving strategies were initialized from different starting points in order to avoid local minimums.

5.4. Post-optimization analyses: Designing actual controller

In this research, two post-optimization analyses were performed. In these analyses, given the optimized process and its control structure, a PI controller was modelled and its tuning parameters were optimized. Such an optimization task has a significantly reduced size because the optimization variables only consist of continuous tuning parameters of the controller. The objective function of this optimization was equation (16) which concerns only the controller error.

In these analyses, the disturbance scenarios described in the fifth and sixth parts of the results of Flores-Tlacuahuac and Biegler (2007) were considered. In addition, similar bounds on the optimization variables were imposed (i.e., $0 < K_p < 500$ and $0 < K_i < 500$). The aim was to provide the opportunity to compare the results of the proposed optimization framework using a dynamic inversely controlled process model and the conventional optimization framework using a combined process-controller model.

5.5. Implementation considerations

As explained in Section 3, two solving strategies were implemented in the present research. The first solving strategy was a sequential dynamic optimization. The embedded algebraic equation (AE) solver and the embedded differential algebraic equation (DAE) solver in Fig. 3 were both implemented in Aspen Custom Modeller (ACM®), which was invoked in steady-state and dynamic modes, respectively. The optimization algorithm was a nonlinear gradient-based solver which was coded in the Visual Basic Application (VBA) environment. The two software tools were linked using Microsoft COM interface. The required programming techniques can be found in the software documentation, (Aspen Custom Modeler documentation 2004). The number of the optimization variables was five in addition to three enumeration variables. The execution time of each optimization iteration was about 30s and the execution time was in the order of several hours for each enumeration. The sequential strategy was applied to the objective function (22) only for the weighting factors $w'_1 = 1$, $w'_2 = 10^{-3}$ due to long execution time.

The second solving strategy was a large MINLP optimization implemented in General Algebraic Modeling System (GAMS®). The total number of optimization variables for the two disturbance scenarios was 7673 of which only three variables are binary and the rest are continuous. A comparison between different MINLP solvers is not the focus of this research but was presented by Flores-Tlacuahuac and Biegler (2007). In this research, the MINLP solvers were DICOPT and SBB (similar to Flores-Tlacuahuac and Biegler 2007). For each combination of weighting factors, the optimization was initialized from several different starting points to avoid local optimums.

The execution time of the full discretization strategy is significantly lower compared to the sequential strategy for two reasons. Firstly, the optimization solver and dynamic model are implemented in the same software. Secondly, while the full discretization strategy traverses an infeasible optimization path, the sequential optimization strategy only examines feasible solutions. The shorter execution time of full discretization provides the opportunity to examine the objective function (22) for a variety of weighting factors, w'_1 and w'_2, as shown in Table 4 and discussed in Section 7.1.3.

The post-optimization analyses (described in Section 5.4) were performed using the built-in optimizer of gPROMS. Here, there are only two optimization variables (i.e., the parameters of the PI controller) and the execution time was less than few minutes.

6. Results

This section presents the results. Table 3 reports the enumeration results of the sequential integration strategy. Each column represents a process and its control structure. All results are reported for the weighting factors $w'_1 = 1$, $w'_2 = 10^{-3}$ in the objective function. However, each column in Table 4 represents the results for different combination of weighting factors, w'_1 and w'_2. Table 5, presents the results of the post-optimization analyses. As discussed in Section 5.4, firstly, a PI controller was designed for the optimal process and control structure (Structure 6 in Table 3), and then its control performance is compared to the results of the conventional optimization framework by Flores-Tlacuahuac and Biegler (2007).

Figs. 5-9 present the graphical results. They are:

- Figs. 5a-c are the time trajectories of the optimal design using the sequential integration strategy, corresponding to Structure 6 in Table 3.
- Figs. 6a-b explain the uncontrollable structures in Table 3. These are the structures where the flowrate of the cooling water was selected as the manipulated variable and the temperature of the first reactor was selected as the controlled variable.
- Fig. 7 shows the effects of the feed temperature on the product composition for two feed compositions.
- Fig. 8 shows the Pareto front for the multi-objective function (22).
- Figs. 9a-c presents the results of the post-optimization analyses as described in Section 5.4. These results correspond to the second and fourth rows in Table 5.

Please cite the following paper at:
Sharifzadeh M, Thornhill NF, (2013). Integrated design and control using a dynamic inversely controlled process model. *Computers & Chemical Engineering*, 48, 121–134. (Link).

Table 3.
The results of optimization for different process and control structures

	Structure 1: Counter-current T_2-T_f	Structure 2: Counter-current T_1-T_f	Structure 3: Counter-current T_2-Q_c	Structure 4: Counter-current T_1-Q_c	Structure 5: Co-current T_2-T_f	**Structure 6: Co-current T_1-T_f**	Structure 7: Co-current T_2-Q_c	Structure 8: Co-current T_1-Q_c
Objective value	3.9402	3.8650	24.2837	-	5.3060	**3.855**	20.305	-
w'_1	1	1	1	1	1	**1**	1	1
w'_2	10^{-3}	10^{-3}	10^{-3}	10^{-3}	10^{-3}	**10^{-3}**	10^{-3}	10^{-3}
Constraint violation	No	No	Yes(2)	Yes(1)	No	**No**	Yes(2)	Yes(1)
Y_p	0	0	0	0	1	**1**	1	1
Y_{cv}	0	1	0	1	0	**1**	0	1
Y_{mv}	0	0	1	1	0	**0**	1	1
$V_1(\text{m}^3)$	2.283	0.971	2.555	-	2.297	**0.968**	2.700	-
$V_2(\text{m}^3)$	1.206	0.782	2.455	-	1.686	**0.780**	2.700	-
$V_{c1}(\text{m}^3)$	0.050	0.050	0.050	-	0.050	**0.050**	0.050	-
V_{c2} (m^3)	0.050	0.050	0.0556	-	0.050	**0.050**	0.050	-
$CV_{setpoint}$ (K)	474.9	500	440	-	470.2	**500**	439.8	-

Y_p represents the structural decision for the cooling system: $Y_p = 0$ counter-current and $Y_p = 1$ co-current. Y_{cv} represents the structural decision for the controlled variables: $Y_{cv} = 0$, i.e., T_2 is CV and $Y_{cv} = 1$, i.e., T_1 is CV. Y_{mv} represents the structural decision for the manipulated variables: $Y_{mv} = 0$, i.e., T_f is MV and $Y_{mv} = 1$, i.e., Q_c is MV. (1) Inversion of the process is not possible (See Figs. 6a-b.). (2) The maximum allowable temperature of the cooling water leaving the process is violated.

Table 4.
The results of optimization for different weighting factors (w'_1, w'_2) in the objective function (22)

	Structure: Co-current T_1-T_f	**Structure: Co-current T_1-T_f**	Structure: Co-current T_1-T_f	Structure: Co-current T_1-T_f	Structure: Co-current T_1-T_f
Objective value	1.0147	**3.8553**	6.8721	9.1727	14.4241
Control objectives	1.00915	**1.9527**	3.0588	3.8637	3.9241
Process objectives	5550	**1902.6**	1271.1	1061.8	1050
w'_1	1	**1**	1	1	1
w'_2	10^{-6}	**10^{-3}**	3×10^{-3}	5×10^{-3}	10^{-2}
Constraints violation	No	**No**	No	No	No
Y_p	1	**1**	1	1	1
Y_{cv}	1	**1**	1	1	1
Y_{mv}	0	**0**	0	0	0
$V_1(\text{m}^3)$	2.700	**0.970**	0.571	0.450	0.450
$V_2(\text{m}^3)$	2.700	**0.783**	0.551	0.462	0.450
$V_{c1}(\text{m}^3)$	0.050	**0.050**	0.050	0.050	0.050
$V_{c2}(\text{m}^3)$	0.050	**0.050**	0.050	0.050	0.050
$CV_{setpoint}(K)$	500	**500**	500	500	500

Please cite the following paper at:

Sharifzadeh M, Thornhill NF, (2013). Integrated design and control using a dynamic inversely controlled process model. *Computers & Chemical Engineering*, 48, 121–134. (Link).

Table 5.

The results of post-optimization: designing a PI controller for the best solution and comparison with the results of Flores-Tlacuahuac and Biegler (2007)

Disturbance	Process and control structure	K_p	K_i	Objective function of Equation (16)
C_f=0.6-0.55	Structure 6 in Table 3	500	500	3.2489×10^{-8}
C_f=0.6-0.55	Case 5 in Table 5 of (Flores-Tlacuahuac and Biegler 2007)	500	500	0.0009
C_f=0.6-0.65	Structure 6 in Table 3	500	500	3.2491×10^{-8}
C_f=0.6-0.65	Case 6 in Table 5 of (Flores-Tlacuahuac and Biegler 2007)	356	500	0.0025

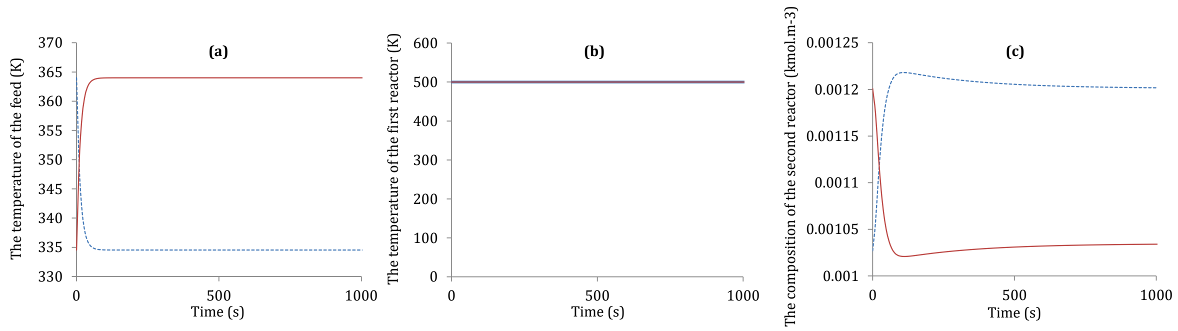

Figs. 5. Results for two disturbances ($w'_1 = 1, w'_2 = 10^{-3}$). Trajectories of a) the feed temperature as the manipulated variable, b) the temperature of the first reactor as the controlled variable (overlaid on each other), c) the composition in the second reactor, using a dynamic inversely controlled process model. Disturbances are a step function from $C_f = 0.55$ to 0.65 (solid line) and $C_f = 0.65$ to 0.55 (dotted line).

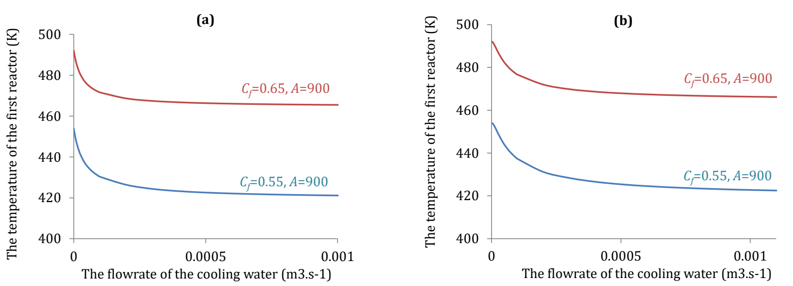

Figs. 6. The variation of the temperature of the first reactor with the flowrate of the cooling water, for a) the co-current structure, b) the counter-current structure.

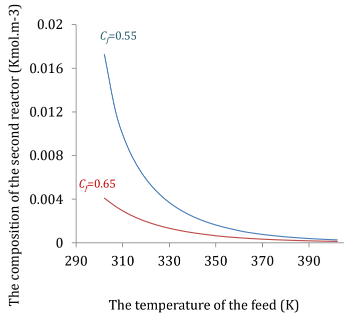

Fig. 7. The variation of the composition of the second reactor with the feed temperature for the co-current structure.

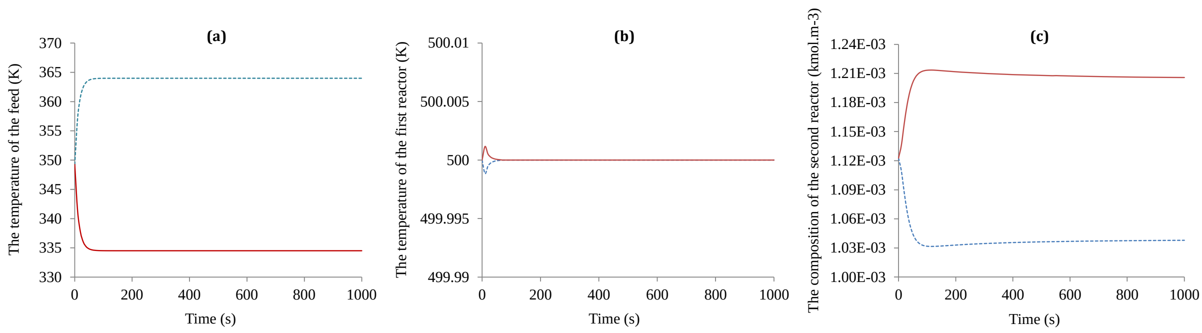

Figs. 9. Results of post-optimization analyses. Trajectories of a) the feed temperature as the manipulated variable, b) the temperature of the first reactor as the controlled variable, c) the composition in the second reactor, using an optimized PI controller. Disturbances are step functions from $C_f =$ 0.6 to 0.55 (dotted line) and $C_f = 0.6$ to 0.65 (solid line) corresponding to case 5 and case 6 of (Flores-Tlacuahuac and Biegler 2007) respectively.

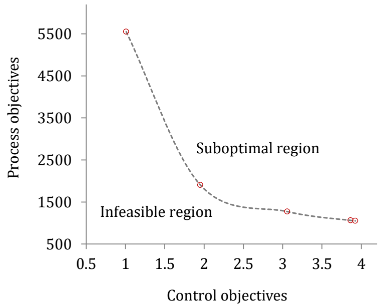

Fig. 8. The Pareto front for the multi-objective function (22) corresponding to the results in Table 4.

7. Discussion

The discussion is presented is two parts. The first part (Section 7.1) discusses the results of the new optimization framework for integrated design and control. The second part (Section 7.2) discusses the physical implication of a dynamic inversely controlled process model by investigating the implication of high index inversed DAEs and the potential causes of imperfect control.

7.1. Discussions of the case study results

In the subsequent sub-sections, firstly the results of the proposed integrated design and control framework are discussed and then the trade-off between the competing and conflicting process and control objectives are explored. The last sub-section also presents a post-optimization analyses and the comparisons between the proposed and the conventional optimization frameworks.

7.1.1. The results of the proposed optimization framework

Table 3 and Table 4 show the results of the sequential integration and full discretization solving strategies, respectively. The third column of Table 4 has the same combination of weighting factors and is equivalent to the seventh column of Table 3. The results of the two solving strategies are in good agreement within the error tolerance of two solving strategies. Table 4 is used for illustrating the relative importance of the control objectives and the process objectives and is discussed later in Section 7.1.3. Table 3 shows the enumeration results of the sequential strategy. The best process and control structure is the structure 6 in which the temperature of the first reactor, T_1 , is the controlled variable and the feed temperature, T_f, is the manipulated variable. The process structure is co-current. A close objective value is also achieved by the structure 2 which has similar control structure but counter-current process structure. In general, counter-current heat exchangers are preferred to co-current heat exchangers. This is because in a counter-current structure, the temperature difference which is the driving force for heat transfer, is kept alive. However, in the case of two series reactors, heat generated by the reaction enhances the temperature difference and maintains the driving force. Therefore, the counter-current structure is not necessarily dominant. The co-current structure has the desirable feature that the effects of the disturbances in the process side (reactor) and the utility side (cooling jacket) move in the same direction and leave the system together, while in the counter current structure, disturbances in process and utility sides move in the opposite directions and remain in the process for a longer period.

The optimal trajectories of the feed temperature as the manipulated variable are shown in Fig. 5a. They show a fast and smooth response. The optimal trajectories of the temperature of the first reactor as the controlled variable are shown in Fig. 5b. These temperature trajectories are two straight lines which are overlaid on each other and imply perfect control. The optimal trajectories of the composition of the second reactor are shown in Fig. 5c. Features of interest are high conversion and very small changes caused by the disturbances, as shown by the small scale of the vertical axis in Fig. 5c.

7.1.2. Uncontrollable process structures

During solving of the optimization, two uncontrollable structures were detected. In those structures, the flow rate of the cooling water was the manipulated variable and the temperature of the first reactor was the controlled variable. These uncontrollability issues manifested themselves as the failure of the integrator of the DAE solver. Fig. 6a gives the explanation. It shows two steady-state analyses which illustrate the variations of the temperature of the first reactor with the flowrate of the cooling water. The cooling water flows in a co-current structure. One profile is calculated for $C_f = 0.55$ kmol.m^{-3} (before disturbance), and the other profile is for $C_f = 0.65$ kmol.m^{-3} (after disturbance). Other process variables are at their nominal values (Table 1). If the initial and final steady states are feasible then a horizontal line must exists that connects the two profiles. Unfortunately, such a horizontal tie-line does not exist and the process inversion is not possible. Similar results are shown in Fig. 6b for the counter-current process structure and the same control structure.

7.1.3. The implications of competing process and control objectives

Table 5 reports optimal solutions for a variety of combinations of the weighting factors in the multi-objective functions (22). The aim was to study the relative importance of the control and process objectives. For simplicity, the first weighting factor was maintained constant at $w'_1 = 1$, while the second weighting factor, w_2, was changed from 10^{-6} to 10^{-2} which are the two extremes where the control and process objectives are dominant, respectively. For $w'_2 = 10^{-6}$ the upper bounds of the reactor volumes are active and the optimizer chose to use the largest possible reactor size, as a large reactor is less sensible to the disturbances in the feed composition. On the other extreme, for $w'_2 = 10^{-2}$, the lower bounds of reactor volumes are active and the control objectives are sacrificed in order to minimize the required capital investment. The optimal solutions for larger values of w'_2 are not shown because the multi-objective function becomes severely insensitive to control objectives and multiple solutions with a similar objective value were detected. The concept is shown in Fig. 8. The horizontal axis and the vertical axis show the control and process objectives, respectively. The points below the Pareto front are infeasible designs. The designs corresponding to the points above the Pareto front are not optimal. The Pareto front illustrates the trade-off between two objectives as improving control objectives requires degrading process objectives, and vice versa, which correspond to moving to left and right on the Pareto front, respectively.

Table 5 also reveals that the process and the control objectives did not compete for the volume of the cooling jackets and the setpoint for the selected controlled variable. The lower bounds are active, because for smaller cooling jackets less investment capital is required and at the same time, the response time of a cooling jacket with smaller hold-up is shorter, hence the process and control objectives point to the same directions. In addition as shown in Fig. 7 and discussed later, a high temperature setpoint for the controlled variables makes the process insensitive to disturbances, while this does not imply any burden for the process objective (as it is defined in this research) and therefore its upper bound is active in all optimal solutions.

7.1.4. Comparison with the results of the conventional optimization framework

As explained in Section 5.4, in order to provide the opportunity for comparing the proposed optimization framework and the conventional framework studied by Flores-Tlacuahuac and Biegler (2007), a set of post-optimization analyses was performed, in which an actual controller was designed for the best solution (Structure 6 in Table 3). Table 5 shows the results of post-optimization. These are equivalent to the fifth and sixth cases studied by Flores-Tlacuahuac and Biegler (2007). The results are also shown graphically in Figs. 9. The small value of the objective function suggests that perfect control is closely pursued by the PI controller. Similar observations can be made from Fig. 9b which shows that the value of the controlled variable is maintained almost constant, (notice the very small scale of the vertical axis).

Another comparison can be made, based on the criteria of inferential control. Controlling the first reactor temperature inferentially aims at controlling the composition of the unconverted reactant in the second reactor and must indirectly attenuate its variations under disturbed conditions. In the conventional optimization framework, for a change of 0.05 kmol.m^{-3} in the feed composition, the composition of the second reactor varies in the range of 0.002 kmol.m^{-3} (Fig. 10 of Flores-Tlacuahuac and Biegler 2007). The variation in the product composition is 4% of the variation in the feed composition. However, using the proposed integrated design and control framework, for the same changes in the feed composition, the composition of the second reactor varies by 0.0001 kmol.m^{-3} (shown in Fig. 9c). Here, the attenuation of the disturbances is about twenty times greater than the conventional method. However, the superior performance of the new integrated design and control framework should be attributed to the term, obj_1, in the objective function (22) which explicitly considers the task of inferential control. Fig. 7 provides the explanation. This figure shows the variations of the second reactor composition with the feed temperature. The top profile is when the feed composition is $C_f = 0.55$ kmol.m^{-3} and the bottom profile is when the feed composition is $C_f = 0.65$ kmol.m^{-3}. Other process variables are at their nominal values (Table 1). The area between these two profiles is the operating region. This figure reveals that by increasing the feed temperature, the composition of the second reactor becomes insensitive to the disturbances in the feed composition, resulting in tighter control and greater attenuation. Since the new framework was successful in recognizing the effects of the feed temperature (manipulated variable), it chose a higher feed temperature (about $30K$ higher than the results of Flores-Tlacuahuac and Biegler 2007). These observations suggest that the control error (equation 16 considered by Flores-Tlacuahuac and Biegler 2007) may have misled the conventional optimization framework to a local solution.

Finally, as well as producing a well-optimized process and control structure, the new integrated design and control framework has achieved a reduction in the complexity of the problem because the differential and algebraic equations of the controller model are replaced by a set of explicit algebraic perfect control equations. Thus, equations (12-15) are replaced by equations (19, 20) which reduces the number of equations. In addition, due to absence of the controller tuning parameters, the number of the optimization variables is less in the proposed framework (e.g., from 10 to 8 in the small example of this article), which in large-scale industrial problems can be an important advantage.

7.2. Physical implications of a dynamic inversely controlled process model

This section investigates physical implications of a dynamic inversely controlled process model. The features of interest are the implications of high index inversed DAEs and limiting factors of functional controllability.

7.2.1. Index reduction

Inversion of a dynamic model may result in high index differential algebraic equations (DAEs). Therefore, it is pertinent to enquire the physical implication of the high index formulation, which is discussed in the following.

McLellan (1994) showed that the index of a nonlinear inversion problem is equal to $n + 1$ where n is the relative order of the process. The relative order is define as the minimum number of times that a controlled variable should be differentiated in order to generate an explicit relationship between that controlled variable and a manipulated variable. It is notable that relative order has been also applied for control structure selection and as a measure of sluggishness of initial response and influence of manipulated variables on controlled variables, (Daoutidis and Kravaris, 1992b). Nonetheless, the relative order has physical implications which are the hidden constraints that impose additional requirements for consist initialization. McLellan (1994) showed that for a consistent initialization of a nonlinear inverse process with relative order of n, the actual and desired values of the controlled variable and its first $n-1$ time derivatives must be equal at the initial point. The physical implication is that there must be no jump in the process behaviour in order to match the perfect control trajectories. Explaining the implication of these requirements for a consistent initialization benefits from differentiating between *setpoint tracking* and *disturbance rejection*. In the case of setpoint tracking, the value of a controlled variable is going to change from an initial state to a final state. For a consistent initialization, the actual and desired values of the first $n-1$ time derivatives have to be equal to some non-zero values. In practice, it is very difficult to measure the time derivative of a controlled variable accurately. Therefore, perfect setpoint tracking is of limited application. However, for disturbance rejection, the time derivatives of controlled variables are all zero because the controlled variables are maintained constant, and index reduction poses no limitation on perfect disturbance rejection. The present paper focused on the disturbance rejection in which the index of the inverse model does not limit the application.

7.2.2. Functional controllability

As explained in the introduction, process inversion guarantees functional controllability. Russell and Perkins (1987) summarized the scenarios in which the inversion of a process model is limited. These are manipulated variables constraints, model uncertainties, time delays, and right-half-plane zeros, which are discussed in the following.

Manipulated variables and their constraints are explicitly included in the optimization formulation and its objective function (Equation 22) and should not be of concern. In addition, a variety of methods for steady-state (Swaney and Grossmann 1985) and dynamic (Dimitriadis and Pistikopoulos 1995; Bansal, et al. 2000) flexibility analysis are available to explore the effects of uncertain parameters, which can be combined with the proposed modelling approach in this paper.

Application of perfect control to processes with time delays needs more care, because handling time delays using process inversion requires prediction. For instance, Perkins and Wong (1985) showed that for a multi-variable linear system the period that must be waited before the controlled variable trajectories can be specified independently, is bounded by the smallest and largest time delays in the process transfer function. The advantage of the proposed methodology is that it does not make any pre-assumption regarding the controller type and predictive (i.e., feedforward) elements can be included in the control law to approach perfect control.

Right half plane zeros in process inversion become poles. Unstable zero dynamics are nonlinear analogue of right half plane zeros, and imply instability of the process inversion, called non-minimum phase behaviour (Slotine and Li 1991). The advantage of incorporating inversion of the process model in the optimization framework is that if a candidate solution is not minimum phase, instability of that solution would result in violation of the constraints and/or an increase in the value of the objective function, which redirects the optimization algorithm towards other candidates that are minimum phase. However, this is only true for the considered disturbances and the solution may or may not be controllable outside of the range of these disturbances. This is because unlike linear systems, the invertibility of nonlinear systems also depends on the initial states which in the context of the proposed optimization framework depend on the considered disturbances. More discussions about invertibility of nonlinear dynamic systems and its relation to the concept of functional controllability can be found in (Hirschorn, 1979).

In addition to above, active constraints may influence controllability in a profound way. The reason is that in the presence of fast-acting disturbances the operating point has to back-off from active constraints in order to ensure feasible operation. The required retreat from the active constraints imposes economic penalties and depends on the design of the process and its control structure, as discussed by Kookos and Perkins (2004). Therefore, in the case of processes that are prone to fast-acting disturbances, the uncertain parameters representing these disturbances need to be included in the problem formulation and the extent of retreat from active constraints should be optimized in order to minimize the associated economic losses.

8. Conclusion

In this paper, a novel optimization framework for integrated design and control is presented which disentangles the complexities associated with controllers by using the assumption of perfect control. In this framework, instead of a combined model of the process and its controller, an inversely controlled process model is used. The treatment is based on the notion of functional controllability in which the process inputs (the required values of the manipulated variables) are generated from the process outputs (the desired value of the controlled variables) by inversion of the dynamic process model. The use of an inversely controlled process model instead of using a particular parameterization, leads to a better conditioned optimization problem and in principle, reduces the combinatorial complexity of the optimization problem that is trying to arrive at a process design optimal both in terms of economics and controllability.

The proposed methodology was benchmarked on a case study of two heat-integrated series reactors, which was previously studies by Flores-Tlacuahuac and Biegler (2007). Two solving strategies were implemented for dynamic optimization of the new integrated design and control framework. The first solving strategy was based on sequential integration. In this strategy, all process and control structures were enumerated. Each enumeration was posed as a nonlinear optimization problem and a differential algebraic equation (DAE) solver provided objective function information to an NLP optimizer. The model inversion was implemented by parameterizing the controlled variable rather than the manipulated variable. Initial states were calculated using a steady-state inversely controlled process model. The second solving strategy was based on full discretization of time-dependent variables. In this solving strategy, the problem was posed as a large-scale MINLP problem and was solved using conventional MINLP optimization methods. The model inversion was implemented by including perfect control equations in the optimization constraints. The initialization issues were systematically addressed by the continuity equations. Since the second strategy allowed the violation of constraints in the intermediate solutions, it was not limited to a feasible optimization path and its execution time was significantly shorter. The new framework utilized a multi-objective function and explored the trade-off between the process objectives and the control objectives. The results demonstrated the advantage of the proposed framework over the conventional one due to disentangling the complexities of the controllers from the problem.

9. Acknowledgement

Mahdi Sharifzadeh gratefully acknowledges partial financial support from the 2010 and 2011 ISA Educational Foundation scholarships, the Burkett Scholarship and Ure bursary award of Chemical Engineering Department, Imperial College London. Nina F. Thornhill gratefully acknowledges the sponsorship of ABB and the Royal Academy of Engineering for the ABB/RAEng Research Chair in Process Automation at Imperial College London.

10. References

Aspen Custom Modeler documentation. (2004). Aspen Modeler Reference Guide, Aspen Technology.

Avraam, M.P., Shah, N., Pantelides, C.C., (1998). Modelling andoptimisation of general hybrid systems in the continuous time domain. *Computers & Chemical Engineering*, 22 (Supplement), S221-S228.

Avraam, M.P., Shah, N., Pantelides, C.C., (1999). A decomposition algorithm for the optimisation of hybrid dynamic processes. *Computers & Chemical Engineering*, 23 (Supplement), S451-S454.

Bansal, V., Perkins, J. D., Pistikopoulos, E. N., Ross, R., van Schijndel, J. M. G., (2000). Simultaneous design and control optimisation under uncertainty. *Computers & Chemical Engineering,* 24 (2-7), 261–266.

Bansal, V., Sakizlis, V., Ross, R., Perkins, J.D., Pistikopoulos, E.N., (2003). New algorithms for mixed-integer dynamic optimization. *Computers & Chemical Engineering*, 27:647-668.

Biegler, L. T., (2010). *Nonlinear Programming: Concepts, Algorithms, and Applications to Chemical Processes.* Society for Industrial & Applied Mathematics, MOS-SIAM series on optimization, Philadelphia, PA.

Bristol, E., (1966). On a new measure of interaction for multivariable process control. *IEEE Transactions on Automatic Control,* 11 (1), 133-134.

Daoutidis, P., Kravaris, C., (1991). Inversion and zero dynamics in nonlinear multivariable control. *AIChE Journal*, 37 (4), 527–538.

Daoutidis, P., Kravaris, C., (1992a). Dynamic output feedback control of minimum-phase nonlinear processes. *Chemical Engineering Science,* 47 (4), 837–849.

Daoutidis, P., Kravaris, C., (1992b). Structural evaluation of control configurations for multivariable nonlinear processes. *Chemical Engineering Science,* 47 (5), 1091–1107.

Daoutidis, P., Kravaris, C., (1994). Dynamic output feedback control of minimum-phase multivariable nonlinear processes. *Chemical Engineering Science,* 49 (4), 433–447.

Dimitriadis, V., Pistikopoulos, E. N., (1995). Flexibility analysis of dynamic systems. *Industrial & Engineering Chemistry Research,* 34, 4451–4462.

Downs, J. J., Skogestad, S., (2011). An industrial and academic perspective on plantwide control. *Annual Reviews in Control*, 35, 99–110.

Flores-Tlacuahuac, A., Biegler, L. T., (2007). Simultaneous mixed-integer dynamic optimization for integrated design and control. *Computers & Chemical Engineering*, 31 (5-6), 588-600.

Garcia C. E., Morari, M., (1982). Internal model control. 1. A unifying review and some new results. *Industrial & Engineering Chemistry Process Design and Development*, 21 (2), 309.

Halvorsen, I. J., Skogestad, S., Morud, J. C., Alstad, V., (2003). Optimal selection of controlled variables. *Industrial & Engineering Chemistry Research*, 42, 3273–3284.

Hangos, K. M., Bokor, J., Szederkényi, G., (2004). *Analysis and Control of Nonlinear Process Systems*. Springer-Verlag, London.

Hirschorn, R., (1979). Invertibility of nonlinear control systems. *IEEE Transactions on Automatic Control,* 24 (6), 855 – 865.

Heath, J. A., Kookos, I. K., Perkins, J. D., (2000). Process control structure selection based on economics. *AIChE Journal*, 46 (10), 1998-2016.

Kookos, I. K., Perkins, J. D., (2004). The back-off approach to simultaneous design and control. In P. Seferlis & M. C. Georgiadis (Eds.), *The Integration of Process Design and Control* (pp. 10–41). Elsevier, Amsterdam, 2004.

Luyben, W. L. (2004). The need for simultaneous design education. In P. Seferlis &M. C. Georgiadis (Eds.), *The Integration of Process Design and Control* (pp. 10–41). Elsevier, Amsterdam, 2004.

Malcolm, A., Polan, J., Zhang, L., Ogunnaike B. A., Linninger A. A., (2007). Integrating systems design and control using dynamic flexibility analysis. *AIChE Journal,* 53 (8), 2048–2061.

McAvoy, T. J., (1999). Synthesis of plantwide control systems using optimization. *Industrial & Engineering Chemistry Research*, 38 (8) 2984–2994.

McAvoy, T.J., Arkun, Y., Chen R., Robinson, D., Schnelle, P.D., (2003). A new approach to defining a dynamic relative gain, *Control Engineering Practice*, 11, 907–914.

McLellan, P. J., (1994). A differential-algebraic perspective on nonlinear controller design methodologies. *Chemical Engineering Science*, 49 (10), l663-1679.

Mohideen, M.J., Perkins, J.D., Pistikopoulos, E.N., (1997). Towards an efficient numerical procedure for mixed integer optimal control. *Computers & Chemical Engineering*, 21 (Supplement), S457-S462.

Morari, M., (1983). Design of resilient processing plants-III: A general framework for the assessment of dynamic resilience. *Chemical Engineering Science,* 38(2), 1881-1891.

Morari, M., Zafiriou, E., (1989). *Robust Process Control*, Prentice-Hall International, Englewood Cliffs, New Jersey.

Narraway, L. T., Perkins, J. D., (1993). Selection of process control structure based on linear dynamic economics. *Industrial & Engineering Chemistry Research*, 1993, 32 (11), 2681–2692, DOI: 10.1021/ie00023a035.

Perkins, j. D., Wong, M. P. F., (1985). Assessing controllability of chemical plants. *Chemical Engineering Research & Design*, 63, 358-362.

Qin, S. J., Badgwell, T. A., (2003). A survey of industrial model predictive control technolog. *Control Engineering Practice*, 11(7), 733-764.

Rawlings, J. B., Stewart, B. T., (2008). Coordinating multiple optimization-based controllers: New opportunities and challenges. *Journal of Process Control*, 18 (9), 839-845.

Russell, L. W., Perkins, J. D., (1987). Towards a method for diagnosis of controllability and operability problems in chemical plants. *Chemical Engineering Research & Design*, 65, 453-461.

Sakizlis, V., Vakamudi, K., Coward, A. , Mermans, I. (2010). Advanced process control in the plant engineering and construction phases. *Hydrocarbon Processing*, October 2010.

Seferlis P., Georgiadis M. C., (2004). *The Integration of Process Design and Control*. Elsevier, Amsterdam.

Schweiger, C. A., Floudas, C. A., (1997). Interaction of design and control: Optimization with dynamic models. In *Optimal Control: Theory, Algorithms, and Applications*. Hager, W. W., Pardalos, P. M., Eds.; Kluwer Academic Publishers: Norwell, MA, 388-435.

Sharif, M., Shah, N., Pantelides, C.C., (1998). On the design of multicomponent batch distillation columns. *Computers & Chemical Engineering*, 22, S69-S76.

Sharifzadeh, M., Thornhill, N.F., (2012). Optimal selection of control structures using a steady-state inversely controlled process model. *Computers & Chemical Engineering,* 38, 126–138.

Skogestad, S., Postlethwaite, I., (2005). *Multivariable Feedback Control: Analysis and Design.* 2nd ed., John Wiley & Sons, Chichester.

Skogestad, S., (2009). Feedback: Still the Simplest and Best Solution. *Modeling, Identification and Control*, 30 (3), 149-155, ISSN 1890-1328.

Slotine, J. E., Li, W., (1991). *Applied nonlinear control*, Prentice-Hall, Englewood Cliffs. ISBN 0130408905.

Stephanopoulos, G., Ng, C. (2000). Perspectives on the synthesis of plant-wide control structures. *Journal of Process Control*, 10 (2-3), 97-111.

Swaney, E., Grossmann I. E., (1985). An index for operation flexibility in chemical process design. 1. Formulation and theory. *AIChE Journal*, 31, 621–630.

Tung, L. S., Edgar, T. F., (1981). Analysis of control-output interactions in dynamic systems *AIChE Journal,* 27, (4) 690–693.

Yuan, Z., Chen, B., Zhao, J., (2011). An overview on controllability analysis of chemical processes. *AIChE Journal*, 57 (5), 1185–1201.